Ref. Ares(2022)4005647 - 30/05/2022

Ponderful

PONDS FOR CLIMATE



Deliverable 3.7

Protocol for downscaling EU and global land use data

European Commission

This project has received funding from the European Union's Horizon 2020 Research and Innovation Programme under Grant Agreement No ID 869296

Ponderful Partners:

University of Vic – Central University of Catalonia (Spain) – Prof. Sandra Brucet (PI, Project Coordinator), Dr. Diana van Gent (Project Manager)

IGB im Forschungsverbund Berlin (Germany) – Dr. Thomas Mehner (PI, WP2 co-coordinator)

Katholieke Universiteit Leuven (Belgium) – Prof. Luc De Meester (PI, WP2 coordinator)

Haute Ecole Spécialisée de Suisse occidentale (Switzerland) – Prof. Beat Oertli (PI, WP4 coordinator)

Universitat de Girona (Spain) –Dr. Dani Boix (PI)

Ecologic Institut gemeinnützige GmbH (Germany) – Dr. Manuel Lago (PI)

University College London (UK) –Dr. Carl Sayer (PI)

Middle East Technical University (Turkey) – Prof. Meryem Beklioğlu (PI)

CIIMAR - Interdisciplinary Centre of Marine and Environmental Research (Portugal) –Dr. José Teixeira (PI, WP5 co-coordinator)

Aarhus University (Denmark) – Dr. Thomas A. Davidson (PI)

Uppsala University (Sweden) –Dr. Malgorzata Blicharska (PI, WP1 coordinator)

Bangor University (UK) – Dr. Sopan Patil (PI, WP3 coordinator)

Technical University of Munich (Germany) – Prof. Johannes Sauer (PI)

I.S.A.R.A. – **Institut Supérieur d'Agriculture Rhône-Alpes (France)** – Dr. Joël Robin (PI)

Freshwater Habitats Trust (UK) – Dr. Jeremy Biggs (PI, WP5 co-coordinator)

Universidad de la República (Uruguay) – Prof. Matías Arim (PI, WP3 co-coordinator)

Randbee Consultants SL (Spain) – Juan Arevalo Torres (PI)

Amphi International APS (Denmark) – Lars Briggs (PI)

Ponderful

Authors:
Parinaz Rashidi, Sopan Patil (Bangor University, UK)

Document title: Deliverable 3.7 – Protocol for downscaling EU and global land use data
Document Type: Deliverable

WP No: 3
WP Title: Scenarios and Modelling
WP Lead: BU

Date: 31 May 2022
Document Status: Final version

European Commission

This project has received funding from the European Union's Horizon 2020 Research and Innovation Programme under Grant Agreement No ID869296

Table of Contents

List of Tables

List of Figures

1. Executive Summary

This protocol presents the methodology to downscale global land use projections at the scale of pondscapes. Previous efforts have used the Global biodiversity model for policy support (GLOBIO4) to downscale the global Land Use Harmonization (LUH2) data to discrete land-use grids of 10 arc-seconds resolution (~300 m). Here, we extend the GLOBIO4 model to further downscale the LUH2 land use projections at spatial resolution of 100 m. The following sections present details on the GLOBIO4 model's land-use allocation method, how to pre-process input data, and future land use maps.

2. Introduction

Human land use, particularly its influence on land cover, is a major driver of ecosystem distribution and function, and consequently of ecosystem service delivery. Changes in land use pose a rising threat to natural ecosystems all over the world. Small aquatic ecosystems, such as ponds, are particularly vulnerable, and legislation often fails to preserve them. Many ponds are endangered by development and contamination from the surrounding land, yet little is known about their biodiversity and conservation importance. Changes in land use pose a threat to the biodiversity and ecosystem function of small water bodies. Land cover and land use information is needed at various spatial and temporal scales – from local to global, and from historic records to future models – to analyse the relationship between land use changes and their impacts on biodiversity. At the local and regional levels, such data are also required for spatial planning. Models are essential for quantifying land use changes and evaluating the efficacy of conservation and restoration efforts. Land use and land cover change models are growing in abundance and complexity due to technological advancements and integration of methodologies from other disciplines. Different types of approaches that have been adopted by researchers to model land use change include linear models, regression analysis, flow systems, cellular automata and Markov chains, neural networks, and agent-based models (Azimi Sardari et al., 2019). A common thread running across all models is the need to downscale global, continental, or regional land requirements to more local, spatially explicit, and visually satisfying outputs.

Deriving land use change (LUC) maps at a fine spatial resolution and over large spatial extents can be useful for various purposes (Dendoncker et al., 2006). For instance, land use (LU) patterns have been demonstrated to have an impact on ecological processes (Parker and Meretsky, 2004), community and species distribution (Peppler-Lisbach, 2003), soil organic carbon stocks (Smith et al., 2006) and water cycle (Chen et al., 2019). Downscaling is also necessary for a more accurate assessment of LUC impacts on the biodiversity of natural areas, which are influenced not only on the quantity of LU but also on the spatial configuration of landscapes that define the relative connectivity or isolation of these areas (Wimberly and Ohmann, 2004). Knowing where LUC will occur is important to predict biodiversity threats and propose effective conservation policies (Vale et al., 2021).

LUC has been regarded as a significant component in simulating Earth system dynamics, and LUC inputs at appropriate time steps and spatial resolutions are necessary to match the configuration of Earth system models (ESMs) and the nature of the spatial heterogeneity of Earth system processes (Brovkin et al., 2013; Lawrence et al., 2016). While ground investigation or satellite remote sensing can be used to get recent historical LUC data (Friedl et al., 2002; Hansen et al., 2000; Loveland et al., 2000; Zhang et al., 2003), future LUC projections are mainly based on mathematical models that integrate socioeconomic and other data from different sectors into a coherent framework to simulate the interactions between human and natural systems (Chen et al., 2019). For example, the Global Change Assessment Model (GCAM), which gives LUC projections at the regional–agroecological or water basin level, has been frequently used to investigate future social and environmental scenarios under various climate mitigation measures (Edmonds et al., 1997; Kim et al., 2006). ESMs divide the Earth's surface into a number of grid cells and their forcing data must be provided at the same spatial resolution (Taylor et al., 2012). As a result, spatial downscaling of subregional LUC has become a crucial step in linking models such as GCAM and ESMs to examine the effects of LUC on natural processes and explore the relationships between human and natural systems (Hibbard and Janetos, 2013; Lawrence et al., 2012).

To date, there are only a few global gridded LU datasets that are publicly available for ESM simulations (Vale et al., 2021). One representative example is the Land Use Harmonization dataset version 2 (LUH2), which is the most complete data in terms of time-series and scenarios of climate change (Vale et al., 2021). LUH2 offers a new harmonized set of land-use scenarios that smoothly connects historical land-use reconstructions with eight future projections in the format required for ESMs (Hurtt et al., 2020). LUH2 is a global gridded land-use dataset at 0.25° × 0.25° resolution. It includes estimates of historical land-use change (850-2015) and future projections (2015-2300) that were generated by integrating and harmonizing land-use history with future projections from various of different integrative assessment models (IAMs)

(Jungclaus et al., 2017; Kim et al., 2018; Lawrence et al., 2016; O'Neill et al., 2016). Essentially, LUH2 harmonizes and, at times, downscales LU projections from GCAM or similar models, such as IMAGE11, REMIND-MAGPIE12, MESSAGE-GLOBIOM13, and AIM (Chen et al., 2020).

The first generation of models (LUH1) (Hurtt et al., 2011, 2006) provided harmonized land use data for the years 1500–2100 at 0.5° × 0.5° resolution and projected future land-use land-cover under CMIP5's Representative Concentration Pathways greenhouse gas scenarios (RCPs). The current generation of models (LUH2) (Hurtt et al., 2020) project future land-use land-cover under CMIP6's Shared Socioeconomic Pathways greenhouse gas scenarios (SSPs)(Vale et al., 2021). LUH2 is driven by the most recent SSPs, has a greater spatial resolution (0.25° vs 0.50°), more detailed land-use transitions (12 vs 5 potential land-use states), and increased data-driven constraints than LUH1 (Kim et al., 2018). With annual time steps, LUH2 supports over 100 possible transitions per grid cell per year (e.g., crop rotations, shifting cultivation, agricultural changes, wood harvest) and numerous agricultural management layers (e.g., irrigation, synthetic nitrogen 30 fertilizer, biofuel crops) (Kim et al., 2018). Primary and secondary natural vegetation are divided into forest and non-forest sub-types, pasture is divided into managed pasture and rangeland, and cropland is divided into multiple crop functional types (C3 annual, C3 perennial, C4 annual, C4 perennial, and N fixing crops) in the 12 states of land (Kim et al., 2018) (Table 1).

Table 1. Comparing Land Use Harmonization v2 (LUH2) with LUH v1 (sources: Hurtt et al., 2011, 2020; Kim et al., 2018).

LUH version	LUH v1	LUH v2
Spatial resolution	0.5 degree	0.25 degree
Time steps	Annually from 1500 to 2100	Annually from 850 to 2300
Land use categories	5 categories Primary Secondary Pasture Urban Crop	12 categories Forested primary land (primf) Non-forested primary land (primn) Potentially forested secondary land (secdf) Potentially non-forested secondary land (secdn) Managed pasture (pastr) Rangeland (range)

		Urban land (urban) C3 annual crops (c3ann) C3 perennial crops (c3per) C4 annual crops (c4ann) C4 perennial crops (c4per) C3 nitrogen-fixing crops (c3nfx)
Future	RCPs (4) 2.6 4.5 6.0 8.5	SSPs (6) SSP1-RCP2.6 SSP4-RCP3.4 SSP2-RCP4.5 SSP4-RCP6.0 SSP3-RCP7.0 SSP5-RCP8.5
Land use transitions	< 20 per grid cell per year	>100 per grid cell per year
Improvements		- New shifting cultivation algorithm - Landsat forest/non-forest change constraint - Expanded diagnostic package - New historical wood harvest reconstruction - Agricultural management layers: irrigation, fertilizer, biofuel crops, wood harvest product split, crop rotations, flooded (rice)

Global land-use projections, such as the LUH2 data, have a coarse spatial resolution (0.25°) and tend to underestimate the spatial heterogeneity of land-use patterns at local to regional scales. Therefore, more detailed LULC information is needed for local-scale applications. Although previous studies have attempted the downscaling of LUH2 projections at various spatial resolutions, with the finest resolution achieved by Schipper et al. (2020) who used the Global Biodiversity model for policy support (GLOBIO) to downscale it to 300 m resolution**,** but still a global high-resolution discrete land-use map (100 m or finer) is not currently available. Therefore, in Work Package 3, we have developed a protocol to extend the GLOBIO model to further downscale land use projections at 100 m (and finer) spatial resolution.

The GLOBIO model was developed in cooperation with multiple partners by PBL Netherlands Environmental Assessment Agency and is intended to inform and support policymakers by quantifying global human impacts on biodiversity and ecosystems. The model is linked to PBL's IMAGE model, which is an integrated assessment model that simulates the global environmental effects of human activities (Doelman et al., 2018). The IMAGE-GLOBIO framework has been widely applied to environmental assessments in recent years, including for the Convention on Biological Diversity (CBD) and the Intergovernmental Science-Policy Platform on Biodiversity and Ecosystem Services (IPBES)(Schipper et al., 2020).

This model is capable of downscaling (or spatially allocating) low-resolution land-use data (regional totals or 'claims') to a global high-resolution discrete land-use map that is compatible with the GLOBIO 4 model environment. Specifically, we are downscaling three future Shared Socio-economic Pathway (SSP) scenarios in the LUH2 data, Sustainable Development (SSP1), Regional Rivalry (SSP3), and Fossil-fuelled Development (SSP5), for the 2018 to 2050 period (Table 2). The sustainability scenario is characterized by a relatively low population growth, low consumption due to less resource-intensive lifestyles (e.g., a decrease in meat consumption) and more resource-efficient technologies, combined with improved technologies, increased regulation of land-use change due to expansion of the protected area network, and significant progresses in agricultural productivity, permitting for reforestation (Schipper et al., 2020). High population expansion, resource intensive consumption, low agricultural productivity, and limited regulation of land use change characterize the regional rivalry scenario, resulting in ongoing deforestation. Finally, the fossil-fuelled development scenario is characterized by low population increase, significant economic growth, a consumption-oriented and energy-intense society, and highly intensive agricultural practices that result in reduced deforestation. Following the biodiversity model intercomparison protocol, we mixed the SSPs with climate projections based on the RCPs (Table 2 and Table 3) so that the combinations encompassed a broad range of land use and climate change (Kim et al., 2018).

SSP1 (moderate land use pressure) was linked with RCP2.6 (low level of climate change), SSP3 (high land use pressure) with RCP6.0 (moderate level of climate change), and SSP5 (moderate land use pressure) with RCP8.5 (high level of climate change). The SSP3 x RCP6.0 and SSP5 x RCP8.5 combinations reflect the so-called baseline scenarios, which include only minor or no climate change mitigation policies.

Table 2. Characteristics of SSP scenarios (source: Kim et al., 2018).

	SSP1 Sustainability	SSP3 Regional Rivalry	SSP5 Fossil-fuel Development
Population growth	Relatively low	Low (OECD countries) to high (high fertility countries)	Relatively low
Urbanization	High	Low	High
Equity and social cohesion	High	Low	High
Economic growth	High to medium	Slow	High
International trade and globalization	Moderate	Strongly constrained	High
Land-use regulation	Strong to avoid environmental trade-off	Low with continued deforestation due to agriculture expansion	Medium with slow decline in deforestation
Agricultural productivity	High improvements with diffusion of best practices	Low with slow technology development and restricted trade	Highly managed and resource intensive
Consumption & diet	Low growth in consumption, low meat	Resource-intensive consumption	Material-intensive consumption, meat-rich diet
Environment	Improving	Serious degradation	Highly successful management
Carbon intensity	Low	High	High
Energy intensity	Low	High	High
Technology development	Rapid	Slow	Rapid
Institution effectiveness	Effective	Weak	Increasingly effective
Policy focus	Sustainable development	Security	Development, free market, human capital

Participation of the land-use sector in mitigation policies	Full	Limited	Full
International cooperation for Climate change mitigation	No delay	Heavy delay	Full

Table 3. Characteristics of RCP scenarios (source: Kim et al., 2018).

	RCP2.6 Low emissions	RCP6.0 Intermediate emissions	RCP8.5 High emissions
Radiative forcing	Peak at 3W/m2 before 2100 and decline	Stabilizes without overshooting pathways to 6W/m2 in 2100	Rising forcing pathways leading to 8.5 W/m2 in 2100
Concentration (p.p.m)	Peak at 490 CO2 equiv. before 2100 and then declines	850 CO2 equiv. (at stabilization after 2100)	>1,370 CO2 equiv. in 2100
Methane emission	Reduced	Stable	Rapid increase
Reliance on fossil fuels	Decline	Heavy	Heavy
Energy intensity	Low	Intermediate	High
Climate policies	Stringent	Very modest	No implementation

3. Methods

Study area

The analysis was conducted on Belgium, a small and highly urbanized country in the densely populated region of Western Europe (Vandenbulcke et al., 2009) with an average population density of circa 370 inhabitants per km2 (Beckers et al., 2020). Belgium, despite its small size, contains a lot of geological variation. The Baltic plain is to the north, while the old Hercynian massifs of Central Europe lie to the south. Apart from the Ardennes, the climate is quite warm and moist, allowing for extensive grass growth. Due to the high population density in the North, extensive animal farming has developed (Dendoncker et al., 2007). The best soil conditions can be found in the country's central region, where arable farming is most prevalent. Because most of the country's southern region (particularly the Hautes–Ardennes) has a harsh climate and soils that prevent the development of industrial crops, grasslands and forests are the major LU (Dendoncker et al., 2007).

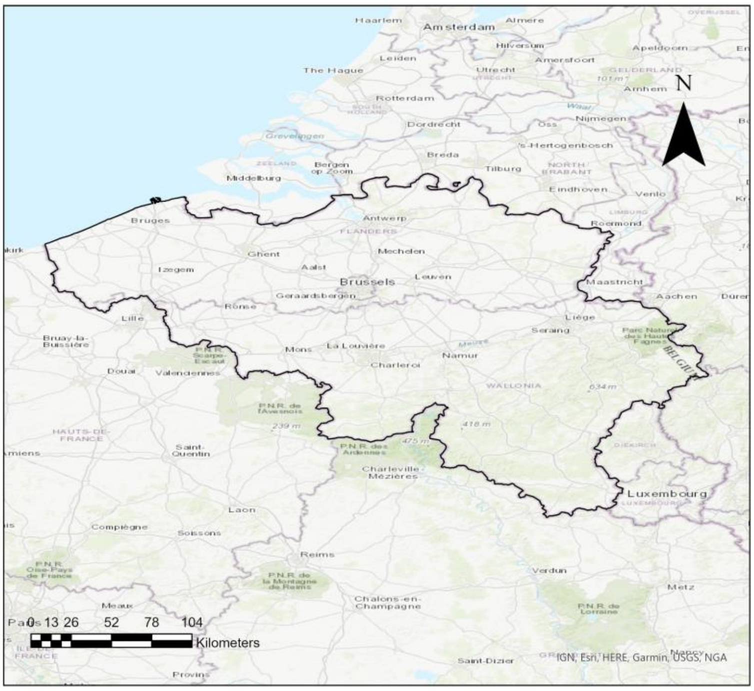

Figure 1. Map of the study area (Belgium).

Globio Land Use Allocation module

Land-use is an important GLOBIO input parameter. The Discrete Land-use Allocation module is a GLOBIO 4 pre-processing module that can be run in the GLOBIO 4 framework. We have extended a routine to downscale land-use data to discrete global maps with a spatial resolution of 5 arc-seconds (100 meter). This improves the ability to account for spatial heterogeneity as well as ecological consequences that are influenced by the landscape's spatial configuration. GLOBIO's land use allocation method can work with user-defined land-use classes and regional totals, or 'claims,' represented in surface area per region per land-use class. Each land-use class's regional totals are spatially allocated based on an overall 'suitability layer' for that class (Schipper et al., 2020). This layer is created using a collection of environmental factors that influence the probability of the land-use class of concern being present in that grid cell. Land cover, road proximity, elevation, and slope are examples of relevant environmental factors (Schipper et al., 2020).

The allocation algorithm prioritizes potential grid cells based on their suitability values and allocates claims for each land use type in each region starting with the cells with the highest suitability and working its way down to the total claim (Schipper et al., 2020). GLOBIO allocates land in a predetermined order, with urban land coming first, followed by cropland, reflecting the fact that urbanization is often prioritized over other land uses (including existing cropland) (d'Amour et al., 2017), and cropland expansion often occurs in forest or grazing land (Piquer-Rodríguez et al., 2018). Following that, forestry and pasture are allocated, with forestry allocating within remaining forest areas and grazing occurring in regions that are not productive enough for crops (Hasegawa et al., 2017). If several cells in a particular region are equally suitable for a certain land use type, the land use claim is distributed among them at random. Claims or changes in claims from the previous scenario–year combinations are assigned to each scenario–year combination. If the land claim allocated in one scenario–year is smaller than the claim allocated in the preceding scenario–year, cells are abandoned in reverse order of suitability and assigned to urban (Schipper et al., 2020).

Land use type

The following land-use types (Table 4) were utilized during the extension process and can be defined in the module's configuration file.

Table 4. Land use types

Code	Type
1	Urban
2	Crop
3	Pasture
4	Forestry
5	Baren
6	Undefined

Data

The following input datasets (Table 5) are used by the extended Land-use Allocation module. Before being utilized as input, many of these datasets are pre-processed. Pre-processing usually included resampling and resizing the original dataset, as well as converting to a tif raster.

Table 5. Input datasets

Type	Description	Data type and range
Regions	Raster with regions	Integer, 0 to 255
Land-cover	Raster with land-cover	Integer, 0 to 255
Land-use	Raster with land-use	Integer, 0 to 255
Not-allocatable areas	Raster with areas which can not be allocated	Integer, 0 = allocatable, 1 = not-allocatable
Suitabilities	Rasters with suitability for the land-use types to allocate.	Floating point, 0.0 (not suitable) to 1.0 (highly suitable)
Land-use claims	File with the claim areas in km2 per region of the land-use types to allocate.	CSV file
Land-use claims lookup	File with the translation of the land-use class in the claim file to the land-use types.	CSV file

The land-use claims file should be in CSV format and contain at least the fields listed below (Table 6).

Table 6. Land-use claims

Type	Description
Land-use	Land-use code or name.
Area	Claim area in km2.

A CSV file with at least the following fields should be specified when a land-use claims lookup file is specified (Table 7).

Table 7. Land-use claims look-up

Type	Description
Land-use class	The land-use class used in the claim file.
Land-use type	The land-use type used in the configuration file.

Input data preparation

Many of these datasets have been pre-processed before being used as input, as detailed below.

Land cover map

We have used Corine land-cover map for the reference year 2018 to establish a baseline land-use map for the present day. The classification system of Corine is different from LUH2, with 12 land use classes in the LUH2 datasets and 44 land use classes in Corine. To make these two datasets comparable for land use simulations, we have merged them into six major classes (forest, pasture, cropland, urban, barren, and water) (Figure 2). Because the change in the amount of water area is not projected in the LUH2 datasets, we assume that water areas do not change under different scenarios and are not simulated in the land use simulation model in this study.

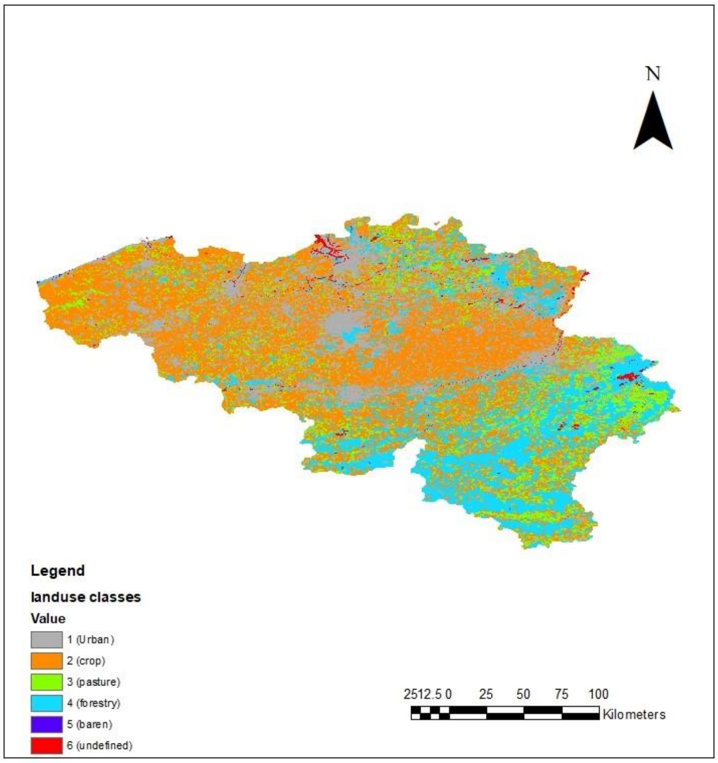

Figure 2. Merged land cover classification into six major land classes for Belgium.

Suitability layers

We created a suitable layer for each of the four major land-use types for compiling the downscaled land-use maps (urban area, cropland, pasture, and forestry) based on the guidelines employed by Schipper et al (2020) for downscaling land use at 300 meters. Because spatial clustering and edge expansion have been identified as significant factors in the growth of urban areas and croplands, we retrieved the suitability layers for urban areas (Figure 3) and croplands (Figure 4) based on their proximity to existing urban areas and croplands (Ay et al., 2017; Huang et al., 2019; Richards, 2018). To that end, we used the Corine land-cover map (after reclassification) to calculate the Euclidean distance to existing urban area (class 1) or croplands (class 2), assign the highest suitability to existing cropland or urban area, and invert and normalize the distances to existing urban area or cropland. We also set the suitability of non-urban and non-cropland cells inside protected areas to zero, based on the assumption that urban and cropland areas within protected areas would not expand beyond what they were in 2018. The World Database of Protected Areas (WDPA) was used to define protected areas.

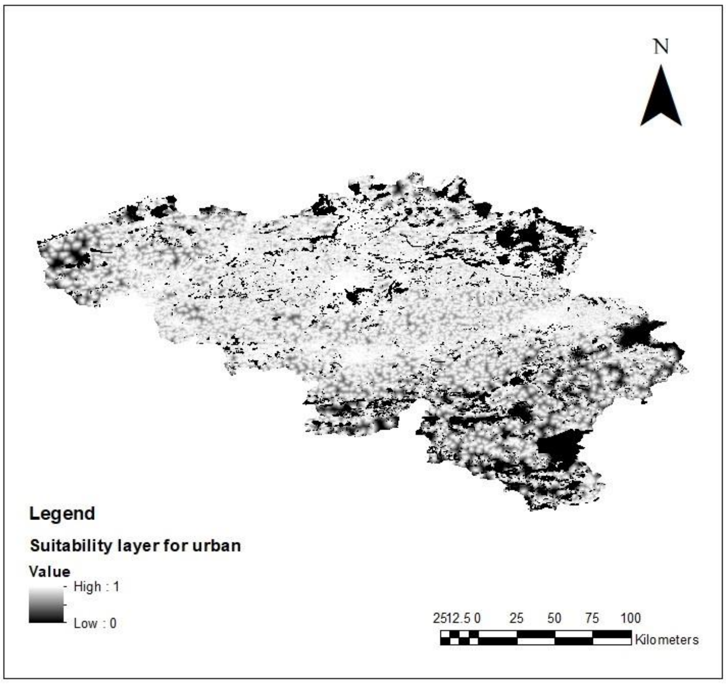

Figure 3. Urban suitability layer for Belgium.

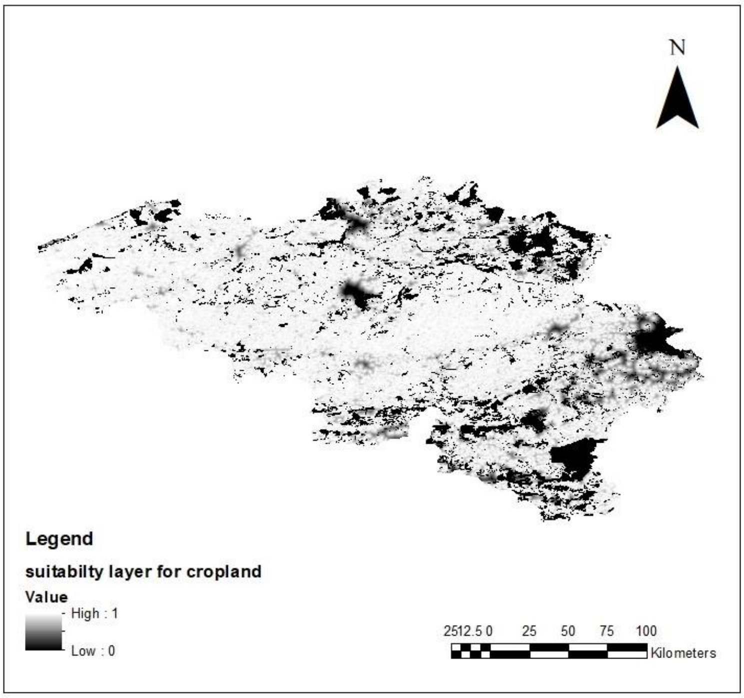

Figure 4. Cropland suitability layer for Belgium.

We created a pasture suitability layer (Figure 5) based on the density of ruminant livestock species (goats, sheep, and cattle) from the FAO's gridded livestock of the world dataset (GLW; head per km2, 30 arc-seconds)(Robinson et al., 2014). Modelled livestock densities are provided by the GLW, which are based on detailed subnational livestock statistics and a set of predictor variables linked to climate, vegetation, topography, and demography (Schipper et al., 2020). To account for variances in body mass among livestock species, we converted their densities to tropical livestock units (Petz et al., 2014).

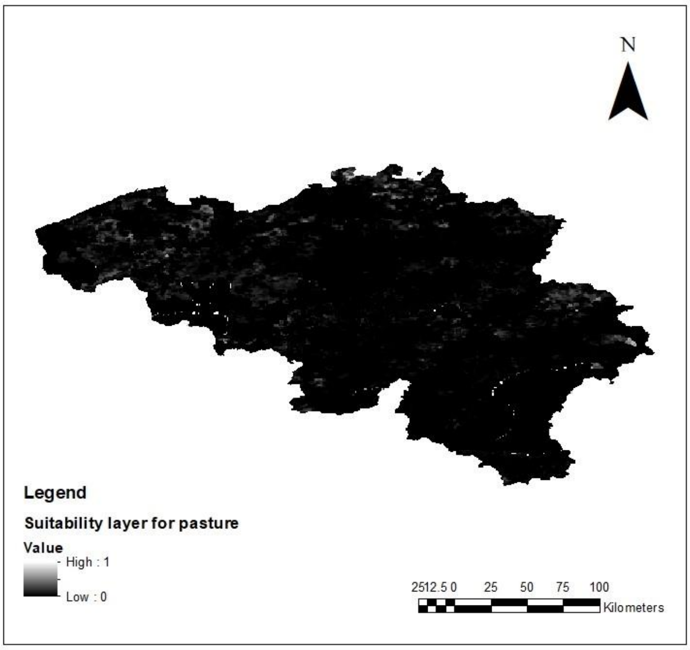

Figure 5. Pasture suitability layer for Belgium.

We considered that access to wood is mostly determined by elevation, proximity to infrastructure, and the presence of protected areas when creating the forestry suitability layer (Schipper et al., 2020) (Figure 6). The Euclidean distance to the nearest road was calculated. We used the GRIP database to get a worldwide road map (Meijer et al., 2018). To get at suitable values between 0 and 1, we inverted and normalized the distances and multiplied the resulting values with inverted and normalized elevation values (retrieved from the Copernicus Land Monitoring Service and resampled to 4 arc-seconds). We also assumed that no forestry activities would take place in protected areas, therefore we set the suitability values for forestry inside protected areas to zero. Finally, we clipped the forestry suitability layer to land cover with trees, using the Corin land cover map for 2018 (classes 4), and set the suitability of other cells to zero.

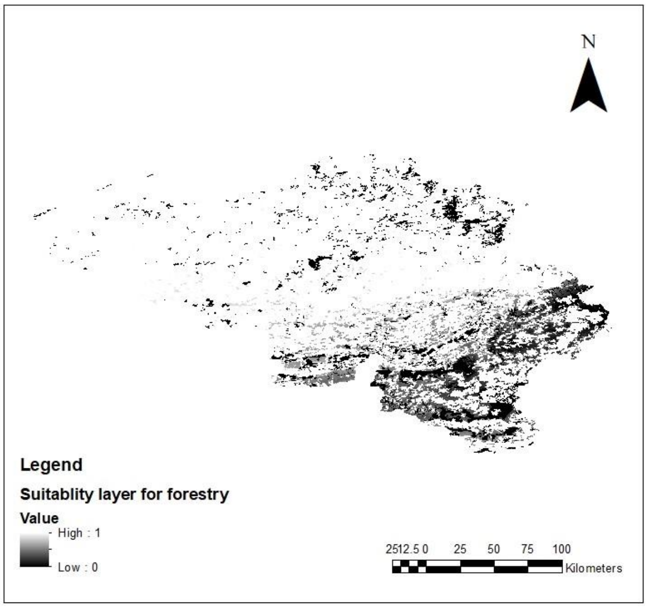

Figure 6. Forestry suitability layer for Belgium.

Claims

Claims can be obtained from national or regional statistics or from models, such as integrated assessment models, that estimate land demand based on socioeconomic developments (Schipper et al., 2020). All claims must be expressed in terms of area (km2). Jelle Hilbers' R algorithm for aggregating LUH data from grid cells to larger regions was utilized and modified. In this code, we have specified three of the shared socio-economic pathways (SSPs) combined with different levels of climate change (according to representative concentration pathways [RCPs]) in the LUH2 data for the 2015 to 2050 period: (SSP1 x RCP2.6), a future determined by a politically divided world (SSP3 x RCP6.0) and a future with continued global dependency on fossil fuels (SSP5 x RCP8.5). This code, on the other hand, is expandable, so you can add other scenarios and time periods to extract claims for different scenarios and dates.

Not-allocatable areas

Not-allocatable areas (Figure 7) were constructed by reclassifying the reclassified land cover map into two classes: allocated areas (Urban, crop, pasture, forestry and barren) and not allocated areas (undefined).

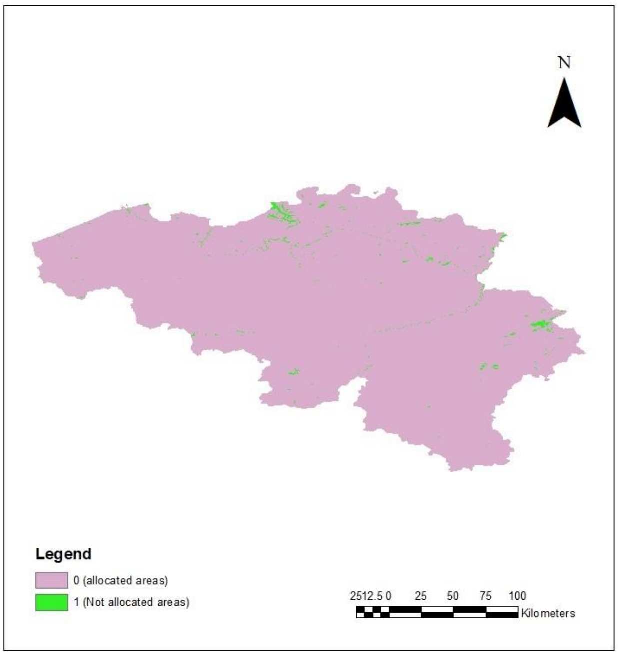

Figure 7. Non-allocatable area map.

Module description

After installing the GLOBIO 4 software (see the installation guide in the https://github.com/GLOBIO4/GlobioModelPublic/wiki), the Land-use Allocation module can be run like any other GLOBIO 4 module using the command globio4. We have provided some detailed information about how to run the model in the sections below.

The following directories in GLOBIO4 are used to create a Raster with allocated land-use.

- Directory – Calculations:

The directory Calculations contains the GLOBIO_CalcDiscreteLanduseAllocation.py which calculates the discrete land-use allocation.

- Directory – Config:

The directory \Config contains the LanduseAllocation.glo which defines the land-use allocation module.

- Directory – LandAllocation

This directory contains additional Python modules used for the Land Use Allocation module. The following Python modules are present: ClaimFile.py which is a class for reading land-use claim files, and LanduseType.py which is a class for storing land-use type information.

- Directory – Scripts

The Directory – Scripts which calculates the global discrete land-use allocation. To define and execute a model run, a script file should contain at least a run definition and a run command. A run definition is an execution block with commands to be executed. The commands can be variable assignments or commands for running other blocks like scenarios, modules or calculations.

Definition of the module

The Land-use Allocation module is defined in the configuration file LanduseAllocation.glo located in the Config directory (PBL Netherlands Environmental Assessment Agency ,2021). The Land-use Allocation module is defined as follows:

```
CalcDiscreteLanduseAllocation(
          IN EXTENT Extent,
          IN CELLSIZE CellSize,
          IN STRING LanduseCodes,
          IN STRING LanduseNames,
          IN STRING LandusePriorityCodes,
          IN RASTER Landcover,
          IN RASTER Regions,
          IN STRING RegionFilter,
          IN STRING RegionExcludeFilter,
          IN RASTER Landuse,
          IN STRING LanduseReplaceCodes,
          IN STRING LanduseReplaceWithCode,
          IN STRING LanduseUndefinedCode,
          IN RASTER NotAllocatableAreas,
          IN RASTER PAReduceFactor,
          IN STRING SuitRasterCodes,
          IN RASTERLIST SuitRasterNames,
```

```
IN FILE ClaimFileName,
IN STRING ClaimLanduseFieldName,
IN STRING ClaimRegionFieldName,
IN STRING ClaimAreaFieldName,
IN FILE ClaimLookup,
IN STRING ClaimAreaMultiplierLanduseCodes,
IN STRING ClaimAreaMultipliers,
IN RASTER CellAreas,
IN BOOLEAN AddNoiseFlag,
OUT FILE OutRegionAreasFileName,
OUT FILE OutRegionLandcoverAreasFileName,
OUT FILE OutRegionLanduseAreasFileName,
OUT RASTER OutAllocatedLanduse)
```

Table 8 below describes the parameters of the Land-use Allocation module.

Table 8. Parameters of the Land-use Allocation module.

Name	Description
Extent	The regional extent, e.g., world.
Cell Size	The cell size, e.g., 4sec.
Land use Codes	The user-defined land-use codes, e.g., 1|2|3|4|5|6.
Land use Names	The user-defined corresponding land-use e.g., urban|crop|pasture|forestry|baren |undefined.
Land use Priority Codes	The sequence in which the land-use codes are allocated, e.g., 1|2|3|4. Not all user-defined land-use codes need to be allocated.
Landcover	Name of raster with land-cover.
Regions	Name of raster with regions.
Region Filter	Selection of region codes which are processed, e.g., 11|12.

	Use NONE for all regions.
Region Exclude Filter	Selection of region codes which are not processed, e.g., 7|16|17. Use NONE for no regions.
Land use	Name of raster with land-use.
Land use Replace Codes	The land-use codes of areas which are not allocated, and which will be replaced with the Land use Replace With Code at the end of the allocation process, e.g. 1|2|3|4.
Land use Replace With Code	The code of the user-defined land-use codes which will be used to fill not-allocated areas at the end of the allocation process, e.g., 5.
Land use Undefined Code	The code of the user-defined land-use codes which will be used to fill areas which could not be allocated, e.g., 6.
Not Allocatable Areas	Name of raster with not-allocatable areas (0 = allocatable, 1 = not-allocatable).
PAReduce Factor	Name of raster with the factors which will be used to reduce the suitability in protected areas (0.0 = high protection, 1.0 = no protection). Use NONE for no raster with protected areas.
Suit Raster Codes	The corresponding land-use codes for the Suit Raster Names, e.g., 1|2|3|4.
Suit Raster Names	The names of the suitability rasters for the land-use types. The suitability varies from 0.0 (not suitable) to 1.0 (highly suitable).
Claim File Name	The name of the csv file with land-use claims (km2) per region per land-use type.
Claim Land use Field Name	The name of the field with the land-use type in the claim file.
Claim Region Field Name	The name of the field with the region code in the claim file.

Claim Area Field Name	The name of the field with the claim area in the claim file
Claim Look up	The lookup file to translate land-use classes in land-use names. Use NONE if no translation is needed.
Claim Area Multipliers	The corresponding land-use codes for the Claim Area Multipliers, e.g., 1|2|3|4.
Claim Area Multiplier Land-use Codes	A list of factors which will be multiplied with the corresponding land-use claim area, e.g. 2.0|4.0|1.0|0.5.
Cell Areas	Name of raster with cell areas (km2).
Add Noise Flag	Flag which can be used to add semi-random noise to the suitability rasters, e.g., TRUE.
Out Region Areas File Name	Name of the file for summarized cell areas per region. Use NONE if no cell areas need to be calculated.
Out Region Land use Areas File Name	Name of the file for summarized cell areas per region per land-use type. Use NONE if no cell areas need to be calculated.
Out Allocated Land use	Name of raster with the new allocated land-use.

Starting a run within Windows

In Windows, open the command window and go to the directory where GLOBIO 4 is installed (for example C:\Python27\Globio4). Type the following command:

cd \Python27\Globio4\Scripts

Create your own configuration script or edit the existing configuration file Run_LanduseAllocation.glo in the directory Scripts. Modify the paths and other settings to meet your needs. To run the script, type the following command.

globio4 Run_LanduseAllocation.glo

After the script is finished the results can be found in the output directory specified in the script.

Calculation rules

The Land-use Allocation module uses the following calculation rules (in pseudo-code) to create a map with allocated land-use types.

- Read the suitability maps for the land-use types to allocate.
- Read the file with land-use claims (km2).
- Optional: translate the land-use classes of the claims to land-use types.
- Read de map with not-allocatable areas.
- Optional: Read the map with the reduce-factors for protected areas.
- Read the map with regions and create a list of region codes. Apply the region filter or the excluded region list. Remove region codes for which there are no land-use claims.
- Read or create a map with raster cell areas in km2.
- Create an empty map for the allocated land-use output (0 = is empty/not yet allocated).
- Read the sequence of land-use types in which they are allocated.
- For all land-use types in this list do:
    - Read the suitability map for this land-use type.
    - Optional: Multiply the suitability with the reduce factor for protected areas.
    - Optional: Add semi-random noise to the suitability map. The minimum difference between all successive suitability values is calculated. For each cell this value is multiplied by a random value between 0.0 and 0.9 which is generated with a fixed seed. This semi-random value is added to the suitability value of that cell.
- For all regions do:
    - Select all cells within the region.
    - Select in here all cells which are allocatable (i.e. not not-allocatable).

- Select in here all cells which are not allocated yet by a previous processed land-use type.
- Sort the remaining cells on suitability from high to low values.
- Get the cell areas of the sorted cells.
- For these cells calculate the cumulative area.
- From this list get the index of the first cell with the cumulative area which is greater or equal to the claim area of the current processed land-use type and region.
- Assign to these cells in the map of allocated land-use the currently processed land-use type.
- Select all empty cells which are allocatable but lie outside the processed regions. Assign the user-defined 'undefined' land-use type to these cells.

- For all processed land-use types do:
  - Select in the allocated land-use map all cells which have in the input land-use map the current land-use type.
  - Select in here all cells which are not allocated yet. Assign to these cells the user-defined 'replace' land-use type e.g. 'secondary vegetation'.
- Read the land-cover map.
- Select all cells which are not allocated yet. Assign to these cells the code from the land-cover type.
- Save the allocated land-use map.
- Optional: Calculate areas.

4. Results

The GLOBIO4 Land-use Allocation module is extended and used to simulate and use changes in Belgium for the period from 2018- 2100. The following output datasets have been calculated.

Present-day land-use map

We used the land-use allocation routine with the reclassified Corine land-cover map for 2018 as the 'background' map, the suitability layers as described above, and country-level total areas (i.e., 'claims') of urban, cropland, pasture, and forestry land to create a land-use map for the reference year 2018 (Figure 8). Like the method of Schipper et al. (2020), we used two data sources to get the most representative claims for 2018: claims for urban area and cropland from the Corine map for 2018 (i.e., the land-cover background map itself) and claims for pasture and forestry (which cannot be distinguished from natural grasslands or natural forest, respectively, based on remotely sensed land-cover maps) from FAOs country-level statistics for 2018. We defined the pasture claim as the total of permanent and temporary meadows at the country level, and the forestry claim as the total of planted forest at the country level. The use of the same source for both the suitability layers and the claims of urban and cropland regions meant that the 'claims' for urban and cropland areas were only assigned to cells identified as such in 2018, i.e., the allocated layers were similar to the Corine map for 2018. As a result, we adhered as near as possible to the claims and patterns identified in 2018.

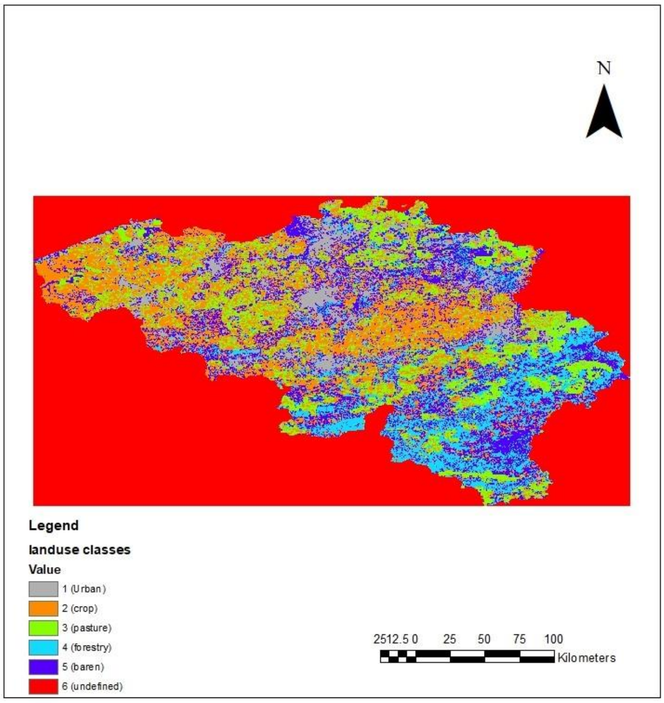

Figure 8. Present day land use map.

Future land-use maps

To create the future land-use maps (Figures 9, 10, and 11), we used the LUH2 dataset to calculate country-level total areas of the four land use types (urban, farmland, pasture, and forestry) for each scenario-year (i.e., 2015 and three times 2050, for each SSP scenario). Because the historical land-use forcing dataset (LUH2 v2) covers the years 850 to 2015, and this year is the closest to 2018, when land use change is negligible, we chose 2015 from the LUH2 historical dataset. We calculated cropland claims as the sum of the areas of the five cropland types included in LUH2 (c3ann + c3per + c4ann + c4per + c3nfx) forestry claims as the sum of wood harvest from forested cells and non-forested cells with primary vegetation (primf harv + primn harv), and pasture claims as the sum of pasture and rangeland areas (Schipper et al., 2020). For each future scenario year, the difference in area of each land-use types relative to 2015 (LUH2 historical dataset) was computed, and the difference was added to the claims defined for 2018 (as mentioned above), with the sum being the overall claim (Schipper et al., 2020). As a result, rather than defining the claims themselves, we used the LUH2 data to define the change in claims, reasoning that the integrated assessment models underlying LUH2 are good at representing temporal trends in land use, but that remote sensing data and national statistics, which were included in our initial land-use map, are better at representing the current situation (Schipper et al., 2020).

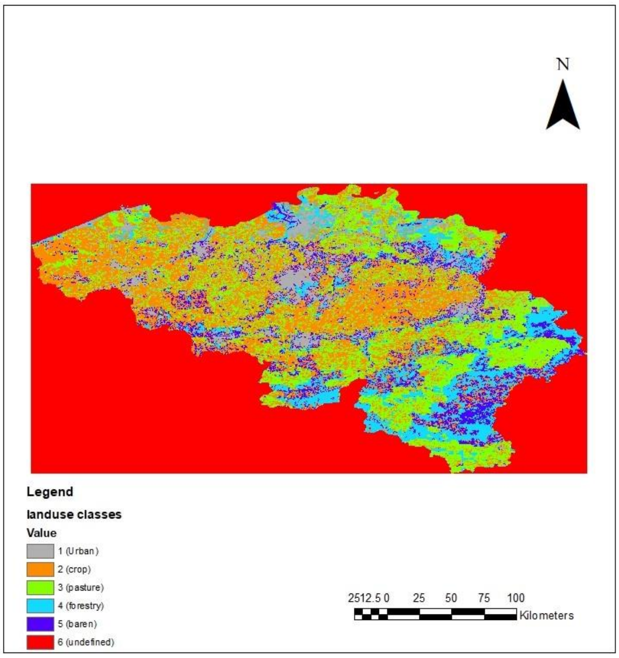

Figure 9. Future land-use map under SSP1 RCP2.6 scenario from 2018 to 2100.

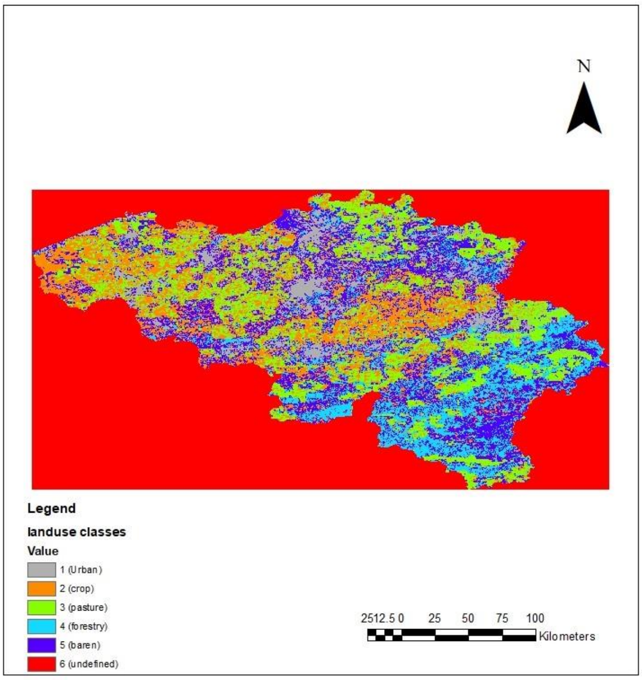

Figure 10. Future land-use map under SSP3 RCP6.0 scenario from 2018 to 2100.

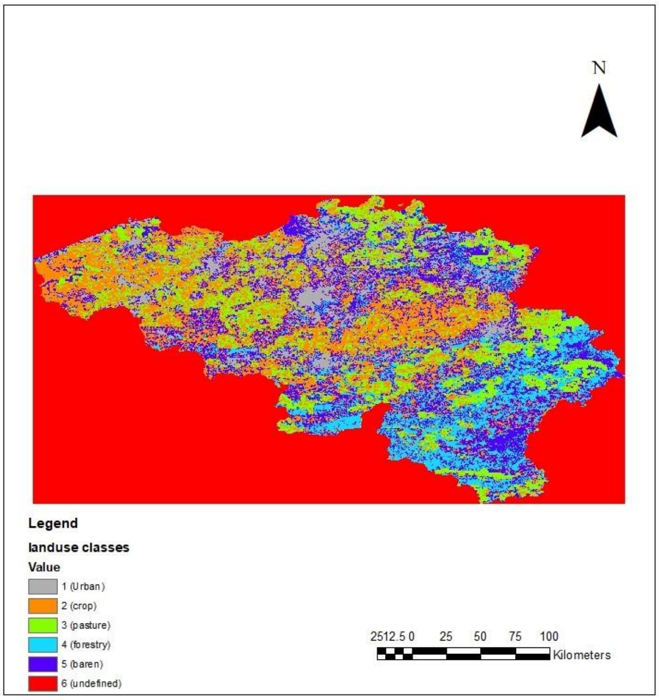

Figure 11. Future land-use map under SSP5 RCP8.5 scenario from 2018 to 2100.

5. Conclusion

Land-use allocation routine of the GLOBIO4 model has been extended to downscale the fractional LUH2 data to discrete land-use grids (5 arc-seconds resolution; ~100 m). To that end, the areas of urban, cropland, pasture, and forestry from LUH2 were first aggregated across the LUH2 grid cells to the national level, with forestry consisting of the wood harvest from forested cells and non-forested cells with primary vegetation. Next, the totals per region were allocated to 100m cells with the GLOBIO4 land allocation routine, with specific suitability layers for urban, cropland, pasture, and forestry. The allocation algorithm then prioritizes candidate grid cells according to their suitability values and allocates the claims of each land-use type in each region starting from the cells with the highest suitability until the total claim is allocated. In the allocation a predefined order is followed, where urban land takes precedence over cropland (d'Amour et al., 2017) and cropland in turn takes precedence over pasture (Hasegawa et al., 2017). If for a given land-use type in a given region there are multiple cells with the same suitability, the allocation is done randomly. Forestry and pasture are allocated thereafter, such that forestry is allocated within remaining forest areas, and reflecting that grazing typically takes place in areas not productive enough for crops (Hasegawa et al., 2017). If for a given land-use type in a given region multiple cells have equal suitability, the land-use claim is distributed randomly among those cells. Claims or changes in claims relative to a preceding scenario– year are allocated per scenario–year combination. If the land claim allocated in a given scenario–year is smaller than the claim allocated in the preceding scenario–year, cells are abandoned in reverse order of suitability and assigned to baren. In this report GLOBIO4 land allocation routine is used at national level for Belgium, the proposed methodology can be used at global, continental, national and landscape levels.

6. Further information

The following data sources were used for running the model.

a) https://land.copernicus.eu/pan-european/corine-land-cover

b) http://luh.umd.edu/data.shtml.

c) https://www.iucn.org/theme/protected-areas/our-work/quality-and-effectiveness/world-database-protected-areas-wdpa

d) https://worldmap.harvard.edu/data/geonode:Digital_Chart_of_the_World

e) https://land.copernicus.eu/imagery-in-situ/eu-dem/eu-dem-v1.1

f) FAO, 2018. FAOSTAT Land domain. http://www.fao.org/faostat/en/#data/RL

g) https://github.com/GLOBIO4/GlobioModelPublic/wiki

All the codes are provided in a GitHub repository.

https://github.com/GLOBIO4/GlobioModelPublic

7. References

Ay, J.-S., Chakir, R., Gallo, J. le, 2017. Aggregated Versus Individual Land-Use Models: Modeling Spatial Autocorrelation to Increase Predictive Accuracy. Environmental Modeling & Assessment 22, 129–145. https://doi.org/10.1007/s10666-016-9523-5

Azimi Sardari, M.R., Bazrafshan, O., Panagopoulos, T., Sardooi, E.R., 2019. Modeling the Impact of Climate Change and Land Use Change Scenarios on Soil Erosion at the Minab Dam Watershed. Sustainability 11. https://doi.org/10.3390/su11123353

Beckers, V., Poelmans, L., van Rompaey, A., Dendoncker, N., 2020. The impact of urbanization on agricultural dynamics: a case study in Belgium. Journal of Land Use Science 15, 626–643. https://doi.org/10.1080/1747423X.2020.1769211

Brovkin, V., Boysen, L., Arora, V.K., Boisier, J.P., Cadule, P., Chini, L., Claussen, M., Friedlingstein, P., Gayler, V., van den Hurk, B.J.J.M., Hurtt, G.C., Jones, C.D., Kato, E., de Noblet-Ducoudré, N., Pacifico, F., Pongratz, J., Weiss, M., 2013. Effect of Anthropogenic Land-Use and Land-Cover Changes on Climate and Land Carbon Storage in CMIP5 Projections for the Twenty-First Century. Journal of Climate 26, 6859–6881. https://doi.org/10.1175/JCLI-D-12-00623.1

Chen, M., Vernon, C.R., Graham, N.T., Hejazi, M., Huang, M., Cheng, Y., Calvin, K., 2020. Global land use for 2015–2100 at 0.05° resolution under diverse socioeconomic and climate scenarios. Scientific Data 7, 320. https://doi.org/10.1038/s41597-020-00669-x

Chen, M., Vernon, C.R., Huang, M., Calvin, K. v, Kraucunas, I.P., 2019. Calibration and analysis of the uncertainty in downscaling global land use and land cover projections from GCAM using Demeter (v1.0.0). Geoscientific Model Development 12, 1753–1764. https://doi.org/10.5194/gmd-12-1753-2019

d'Amour, C.B., Reitsma, F., Baiocchi, G., Barthel, S., Güneralp, B., Erb, K.-H., Haberl, H., Creutzig, F., Seto, K.C., 2017. Future urban land expansion and implications for global croplands. Proceedings of the National Academy of Sciences 114, 8939–8944.

Dendoncker, N., Bogaert, P., Rounsevell, M., 2006. A statistical method to downscale aggregated land use data and scenarios. Journal of Land Use Science 1, 63–82. https://doi.org/10.1080/17474230601058302

Dendoncker, N., Rounsevell, M., Bogaert, P., 2007. Spatial analysis and modelling of land use distributions in Belgium. Computers, Environment and Urban Systems 31, 188–205. https://doi.org/https://doi.org/10.1016/j.compenvurbsys.2006.06.004

Doelman, J.C., Stehfest, E., Tabeau, A., van Meijl, H., Lassaletta, L., Gernaat, D.E.H.J., Hermans, K., Harmsen, M., Daioglou, V., Biemans, H., van der Sluis, S., van Vuuren, D.P., 2018. Exploring SSP land-use dynamics using the IMAGE model: Regional and gridded scenarios of land-use change and land-based climate change mitigation. Global Environmental Change 48, 119–135. https://doi.org/https://doi.org/10.1016/j.gloenvcha.2017.11.014

Edmonds, J., Wise, M., Pitcher, H., Richels, R., Wigley, T., MacCracken, C., 1997. An Integrated Assessment of Climate Change and the Accelerated Introduction of Advanced Energy Technologies - An Application of MiniCAM 1.0. Mitigation and Adaptation Strategies for Global Change 1, 311–339. https://doi.org/10.1023/B:MITI.0000027386.34214.60

Friedl, M.A., McIver, D.K., Hodges, J.C.F., Zhang, X.Y., Muchoney, D., Strahler, A.H., Woodcock, C.E., Gopal, S., Schneider, A., Cooper, A., Baccini, A., Gao, F., Schaaf, C., 2002. Global land cover mapping from MODIS: algorithms and early results. Remote Sensing of Environment 83, 287–302. https://doi.org/https://doi.org/10.1016/S0034-4257(02)00078-0

Hansen, M.C., Defries, R.S., Townshend, J.R.G., Sohlberg, R., 2000. Global land cover classification at 1 km spatial resolution using a classification tree approach. International Journal of Remote Sensing 21, 1331–1364. https://doi.org/10.1080/014311600210209

Hasegawa, T., Fujimori, S., Ito, A., Takahashi, K., Masui, T., 2017. Global land-use allocation model linked to an integrated assessment model. Science of The Total Environment 580, 787–796. https://doi.org/https://doi.org/10.1016/j.scitotenv.2016.12.025

Hibbard, K.A., Janetos, A.C., 2013. The regional nature of global challenges: a need and strategy for integrated regional modeling. Climatic Change 118, 565–577. https://doi.org/10.1007/s10584-012-0674-3

Huang, X., Xia, J., Xiao, R., He, T., 2019. Urban expansion patterns of 291 Chinese cities, 1990–2015. International Journal of Digital Earth 12, 62–77. https://doi.org/10.1080/17538947.2017.1395090

Hurtt, G.C., Chini, L., Sahajpal, R., Frolking, S., Bodirsky, B.L., Calvin, K., Doelman, J.C., Fisk, J., Fujimori, S., Klein Goldewijk, K., Hasegawa, T., Havlik, P., Heinimann, A., Humpenöder, F., Jungclaus, J., Kaplan, J.O., Kennedy, J., Krisztin, T., Lawrence, D., Lawrence, P., Ma, L., Mertz, O., Pongratz, J., Popp, A., Poulter, B., Riahi, K., Shevliakova, E., Stehfest, E., Thornton, P., Tubiello, F.N., van Vuuren, D.P., Zhang, X., 2020. Harmonization of global land use change and management for the period 850–2100 (LUH2) for CMIP6. Geoscientific Model Development 13, 5425–5464. https://doi.org/10.5194/gmd-13-5425-2020

Hurtt, G.C., Chini, L.P., Frolking, S., Betts, R.A., Feddema, J., Fischer, G., Fisk, J.P., Hibbard, K., Houghton, R.A., Janetos, A., Jones, C.D., Kindermann, G., Kinoshita, T., Klein Goldewijk, K., Riahi, K., Shevliakova, E., Smith, S., Stehfest, E., Thomson, A., Thornton, P., van Vuuren, D.P., Wang, Y.P., 2011. Harmonization of land-use scenarios for the period 1500–2100: 600 years of global gridded annual land-use transitions, wood harvest, and resulting secondary lands. Climatic Change 109, 117. https://doi.org/10.1007/s10584-011-0153-2

Hurtt, G.C., Frolking, S., Fearon, M.G., Moore, B., Shevliakova, E., Malyshev, S., Pacala, S.W., Houghton, R.A., 2006. The underpinnings of land-use history: Three centuries of global gridded land-use transitions, wood-harvest activity, and resulting secondary lands. Global Change Biology 12, 1208–1229.

Jungclaus, J.H., Bard, E., Baroni, M., Braconnot, P., Cao, J., Chini, L.P., Egorova, T., Evans, M., González-Rouco, J.F., Goosse, H., Hurtt, G.C., Joos, F., Kaplan, J.O., Khodri, M., Klein Goldewijk, K., Krivova, N., LeGrande, A.N., Lorenz, S.J., Luterbacher, J., Man, W., Maycock, A.C., Meinshausen, M., Moberg, A., Muscheler, R., Nehrbass-Ahles, C., Otto-Bliesner, B.I., Phipps, S.J., Pongratz, J., Rozanov, E., Schmidt, G.A., Schmidt, H., Schmutz, W., Schurer, A., Shapiro, A.I., Sigl, M., Smerdon, J.E., Solanki, S.K., Timmreck, C., Toohey, M., Usoskin, I.G., Wagner, S., Wu, C.-J., Yeo, K.L., Zanchettin, D., Zhang, Q., Zorita, E., 2017. The PMIP4 contribution to CMIP6 – Part 3: The last millennium, scientific objective, and experimental design for the PMIP4 past1000 simulations. Geoscientific Model Development 10, 4005–4033. https://doi.org/10.5194/gmd-10-4005-2017

Kim, H., Rosa, I.M.D., Alkemade, R., Leadley, P., Hurtt, G., Popp, A., van Vuuren, D.P., Anthoni, P., Arneth, A., Baisero, D., Caton, E., Chaplin-Kramer, R., Chini, L., de Palma, A., di Fulvio, F., di Marco, M., Espinoza, F., Ferrier, S., Fujimori, S., Gonzalez, R.E., Gueguen, M., Guerra, C., Harfoot, M., Harwood, T.D., Hasegawa, T., Haverd, V., Havl\'{\i}k, P., Hellweg, S., Hill, S.L.L., Hirata, A., Hoskins, A.J., Janse, J.H., Jetz, W., Johnson, J.A., Krause, A., Leclère, D., Martins, I.S., Matsui, T., Merow, C., Obersteiner, M., Ohashi, H., Poulter, B., Purvis, A., Quesada, B., Rondinini, C., Schipper, A.M., Sharp, R., Takahashi, K., Thuiller, W., Titeux, N., Visconti, P., Ware, C., Wolf, F., Pereira, H.M., 2018. A protocol for an intercomparison of biodiversity and ecosystem services models using harmonized land-use and climate scenarios. Geoscientific Model Development 11, 4537–4562. https://doi.org/10.5194/gmd-11-4537-2018

Kim, S.H., Edmonds, J., Lurz, J., Smith, S.J., Wise, M., 2006. The ObjECTS framework for integrated assessment: hybrid modeling of transportation. The Energy Journal.

Lawrence, D.M., Hurtt, G.C., Arneth, A., Brovkin, V., Calvin, K. v, Jones, A.D., Jones, C.D., Lawrence, P.J., de Noblet-Ducoudré, N., Pongratz, J., Seneviratne, S.I., Shevliakova, E., 2016. The Land Use Model Intercomparison Project (LUMIP) contribution to CMIP6: rationale and experimental design. Geoscientific Model Development 9, 2973–2998. https://doi.org/10.5194/gmd-9-2973-2016

Lawrence, P.J., Feddema, J.J., Bonan, G.B., Meehl, G.A., O'Neill, B.C., Oleson, K.W., Levis, S., Lawrence, D.M., Kluzek, E., Lindsay, K., Thornton, P.E., 2012. Simulating the Biogeochemical and Biogeophysical Impacts of Transient Land Cover Change and Wood Harvest in the Community Climate System Model (CCSM4) from 1850 to 2100. Journal of Climate 25, 3071–3095. https://doi.org/10.1175/JCLI-D-11-00256.1

Loveland, T.R., Reed, B.C., Brown, J.F., Ohlen, D.O., Zhu, Z., Yang, L., Merchant, J.W., 2000. Development of a global land cover characteristics database and IGBP DISCover from 1 km AVHRR data. International Journal of Remote Sensing 21, 1303–1330. https://doi.org/10.1080/014311600210191

Meijer, J.R., Huijbregts, M.A.J., Schotten, K.C.G.J., Schipper, A.M., 2018. Global patterns of current and future road infrastructure. Environmental Research Letters 13, 064006. https://doi.org/10.1088/1748-9326/aabd42

O'Neill, B.C., Tebaldi, C., van Vuuren, D.P., Eyring, V., Friedlingstein, P., Hurtt, G., Knutti, R., Kriegler, E., Lamarque, J.-F., Lowe, J., Meehl, G.A., Moss, R., Riahi, K., Sanderson, B.M., 2016. The Scenario Model Intercomparison Project (ScenarioMIP) for CMIP6. Geoscientific Model Development 9, 3461–3482. https://doi.org/10.5194/gmd-9-3461-2016

Parker, D.C., Meretsky, V., 2004. Measuring pattern outcomes in an agent-based model of edge-effect externalities using spatial metrics. Agriculture, Ecosystems & Environment 101, 233–250. https://doi.org/https://doi.org/10.1016/j.agee.2003.09.007

Peppler-Lisbach, C., 2003. Predictive modelling of historical and recent land-use patterns. Phytocoenologia 33, 565–590.

Petz, K., Alkemade, R., Bakkenes, M., Schulp, C.J.E., van der Velde, M., Leemans, R., 2014. Mapping and modelling trade-offs and synergies between grazing intensity and ecosystem services in rangelands using global-scale datasets and models. Global Environmental Change 29, 223–234. https://doi.org/https://doi.org/10.1016/j.gloenvcha.2014.08.007

Piquer-Rodríguez, M., Butsic, V., Gärtner, P., Macchi, L., Baumann, M., Gavier Pizarro, G., Volante, J.N., Gasparri, I.N., Kuemmerle, T., 2018. Drivers of agricultural land-use change in the Argentine Pampas and Chaco regions. Applied Geography 91, 111–122. https://doi.org/https://doi.org/10.1016/j.apgeog.2018.01.004

Richards, P., 2018. It's not just where you farm; it's whether your neighbor does too. How agglomeration economies are shaping new agricultural landscapes. Journal of Economic Geography 18, 87–110. https://doi.org/10.1093/jeg/lbx009

Robinson, T.P., Wint, G.R.W., Conchedda, G., van Boeckel, T.P., Ercoli, V., Palamara, E., Cinardi, G., D'Aietti, L., Hay, S.I., Gilbert, M., 2014. Mapping the Global Distribution of Livestock. PLOS ONE 9, e96084-.

Schipper, A.M., Hilbers, J.P., Meijer, J.R., Antão, L.H., Benítez-López, A., de Jonge, M.M.J., Leemans, L.H., Scheper, E., Alkemade, R., Doelman, J.C., Mylius, S., Stehfest, E., van Vuuren, D.P., van Zeist, W.-J., Huijbregts, M.A.J., 2020. Projecting terrestrial biodiversity intactness with GLOBIO 4. Global Change Biology 26, 760–771. https://doi.org/https://doi.org/10.1111/gcb.14848

Smith, P., Smith, J., Wattenbach, M., Meyer, J., Lindner, M., Zaehle, S., Hiederer, R., Jones, R.J.A., Montanarella, L., Rounsevell, M., Reginster, I., Kankaanpää, S., 2006. Projected changes in mineral soil carbon of European forests, 1990–2100. Canadian Journal of Soil Science 86, 159–169. https://doi.org/10.4141/S05-078

Taylor, K.E., Stouffer, R.J., Meehl, G.A., 2012. An Overview of CMIP5 and the Experiment Design. Bull Am Meteorol Soc 93, 485–498. https://doi.org/10.1175/BAMS-D-11-00094.1

Vale, M.M., Lima-Ribeiro, M.S., Rocha, T.C., 2021. GLOBAL LAND-USE AND LAND-COVER DATA: HISTORICAL, CURRENT AND FUTURE SCENARIOS. bioRxiv 2021.05.06.442941. https://doi.org/10.1101/2021.05.06.442941

Vandenbulcke, G., Steenberghen, T., Thomas, I., 2009. Mapping accessibility in Belgium: a tool for land-use and transport planning? Journal of Transport Geography 17, 39–53. https://doi.org/https://doi.org/10.1016/j.jtrangeo.2008.04.008

Wimberly, M.C., Ohmann, J.L., 2004. A multi-scale assessment of human and environmental constraints on forest land cover change on the Oregon (USA) coast range. Landscape Ecology 19, 631–646. https://doi.org/10.1023/B:LAND.0000042904.42355.f3

Zhang, X., Friedl, M.A., Schaaf, C.B., Strahler, A.H., Hodges, J.C.F., Gao, F., Reed, B.C., Huete, A., 2003. Monitoring vegetation phenology using MODIS. Remote Sensing of Environment 84, 471–475. https://doi.org/https://doi.org/10.1016/S0034-4257(02)00135-9

Ponderful

Coordinator: Prof. Sandra Brucet, University of Vic – Central University of Catalonia & ICREA

Project Manager: Dr. Diana van Gent, University of Vic – Central University of Catalonia

Contact: diana.vangent@uvic.cat

Duration: 1 December 2020 to 1 December 2024

Website: www.ponderful.eu

Facebook: /Ponderful-331847228188664

Twitter: @ponds4climate